An "on-off-on" fluorescent nanoprobe for recognition of Cu^{2+} and GSH based on nitrogen co-doped carbon quantum dots

Experimental

Materials

D-glucose, L-Asparagine and amino acids containing arginine (Arg), alanine (Ala), cysteine (Cys), methionine (Met), histidine (His), threonine (Thr), proline (Pro), leucine (Leu), lysine (Lys), phenylalanine (Phe), tryptophan (Trp), tyrosine (Tyr), glycine (Gly), aspartic acid (Asp), valine (Val), isoleucine (Ile), serine (Ser) and glutamic acid (Glu) were purchased from Aldrich (Milwaukee, WI, USA). KCl, NaCl, $CaCl_2$, $ZnCl_2$, $BaCl_2$, $MnCl_2$, $AlCl_3$, $CrCl_3$, $AgNO_3$, $Mg(NO_3)_2$, $Cu(NO_3)_2$, $Ni(NO_3)_2$, $Co(NO_3)_2$, $Cd(NO_3)_2$, $Pb(NO_3)_2$, $Hg(NO_3)_2$, $Fe(NO_3)_3$, $FeSO_4$ were obtained from Aladdin Ltd (Shanghai, China). Dimethyl sulfoxide (DMSO), Dulbecco's modified Eagle's medium (DMEM), fetal bovine serum (FBS), trypsin, ethylenediamine tetraacetic acid (EDTA), and 3-(4,5-dimethylthiazol-2-yl)-2,5-diphenyltetrazolium bromide (MTT) were purchased from Solarbio (Beijing, China). Other reagents were taken from Beijing Chemical Reagents Company (Beijing, China). All chemicals used were analytical reagent grade and were used without further purification. In all experiments, the water was treated as ultrapure water (≥18.25 MΩ cm) from a molecular purification system (Shanghai, China)

Determination of QY

The quantum yield Φs of the CDs were determined by a comparative method as follows:

$$\Phi_S = \Phi_R(Grad_S/Grad_R)(\eta_S^2/\eta_R^2)$$

where Grad is the gradient from the plot of integrated fluorescence intensity against absorbance and η (1.33) is the refractive index of the solvent. The subscripts S and R represent CDs and the reference (quinine sulfate in 0.10 M H_2SO_4). To prevent the re-absorption effect, the absorbances of CDs and quinine sulfate solutions in the 10-mm fluorescence cuvette were adjusted to less than 0.10 at the excitation wavelength (λex) of 380 nm (i.e., the absorption maximum of CDs). The integrated fluorescence intensity was the area under the PL curve in the wavelength range 400–700 nm. The ΦR was taken as 0.54 since it is almost independent (within 5%) with λex at 200–400 nm.

Table S1. Elemental analysis of the as-synthesised NCDs.

Sample name	Elemental content (%)			
	C	H	N	O (Calculated)
NCDs	41.5	4.8	9.0	44.7

Table S2. Comparison of detection limit between the proposed fluorescent sensor and

other reported detection methods for Cu^{2+}.

Sensing probe	Method	Response region(μM)	Detection limits (μM)	Reference
TPEA-CDs	Fluorescence	1-100	10.0 nM	[1]
CCDs	Fluorescence	0.7-4.0	0.13 μM	[2]
CD@SiO_2@CdTe	Fluorescence	0.1-1	0.096μM	[3]
CdSe@CDs-TPEA	Fluorescence	0.01–100	1.0μM	[4]
BSA-CDs	Fluorescence	0.002-1.5	1.3ppm	[5]
N-CDs	Fluorescence	0-5	0.09μM	[6]
N-CDs	Fluorescence	0.001-1.1	5.0nM	[7]
N,S-CDs	Fluorescence	10-90	0.18μM	[8]
APTES-CDs	Fluorescence	0.833-833	0.30μM	[9]
Coumarin-Rhodamine B	Colorimetric	0-40	0.50 μM	[10]
EDTA	Capillary electrophoresis	10-500nM	2.7nM	[11]
Carbon Dot-TPEA	Electrochemical	1-60	100 nM	[12]
N-CDs	Fluorescence	0.004-0.1 and 0.6-222	3.62×10^{-4} μM	This work

Table S3. Lifetime calculations from the time-resolved decay profiles of NCDs and NCDs-Cu^{2+}.

Sample	τ1 (ns)	Percentage (%)	τ2 (ns)	Percentage (%)	Ave.τ (ns)
NCDs	1.0177	16.88	5.0324	83.12	4.3547
NCDs-Cu^{2+}	0.9738	17.70	4.9117	36.69	1.9745
NCDs-Cu^{2+}-GSH	0.6214	19.13	4.1478	80.87	3.4732

Table S4. Zeta potential of N-CDs, NCDs-$Cu^{2+}$and NCDs-Cu^{2+}-GSH.

Sample	Zeta potential (mV)
NCDs	-8.59 mV
NCDs-Cu^{2+}	-3.31 mV
NCDs-Cu^{2+}-GSH	-8.32 mV

Table S5. Application of the proposed quenching fluorescence (FL) method for the determination of Cu^{2+}in river water sample spiked with different amounts of Cu^{2+}.

Sample	The quenching FL method				Flame atomic absorption spectrometric method			
	Added (μM)	Found (μM)	R.S.D. (%)	Recovery (%)	Added (μM)	Founda (μM)	R.S.D. (%)	Recovery (%)

1	20	20.4	3.5	100.2	20	19.8	3.1	99.0
2	40	39.8	4.6	99.5	40	41.3	2.1	103.2
3	80	80.1	3.1	100.1	80	80.4	3.8	100.5

Table S6. Comparison of detection limit between the proposed fluorescent sensor and other reported detection methods for GSH.

Sensing probe	Method	Response region(μM)	Detection limits	Reference
CDs/AuNP	Absorption	0.001-4	50 nM	13
CDs@MS	Photoelectrochemical	0.02-4.0	6.2 nM	14
CDs-Cu^{2+}	Fluorescence	0.1-11	86 nM	4
CDs-MnO_2	Fluorescence	1–10	300 nM	15
N-CQDs-RhB-Hg^{2+}	Fluorescence	0.08-60	20 nM	16
CDs	Fluorescence	0.2-1000	20 nM	17
NCDs-Cu^{2+}	Fluorescence	0.003-0.33 and 1-154	6.32×10^{-4} μM	This work

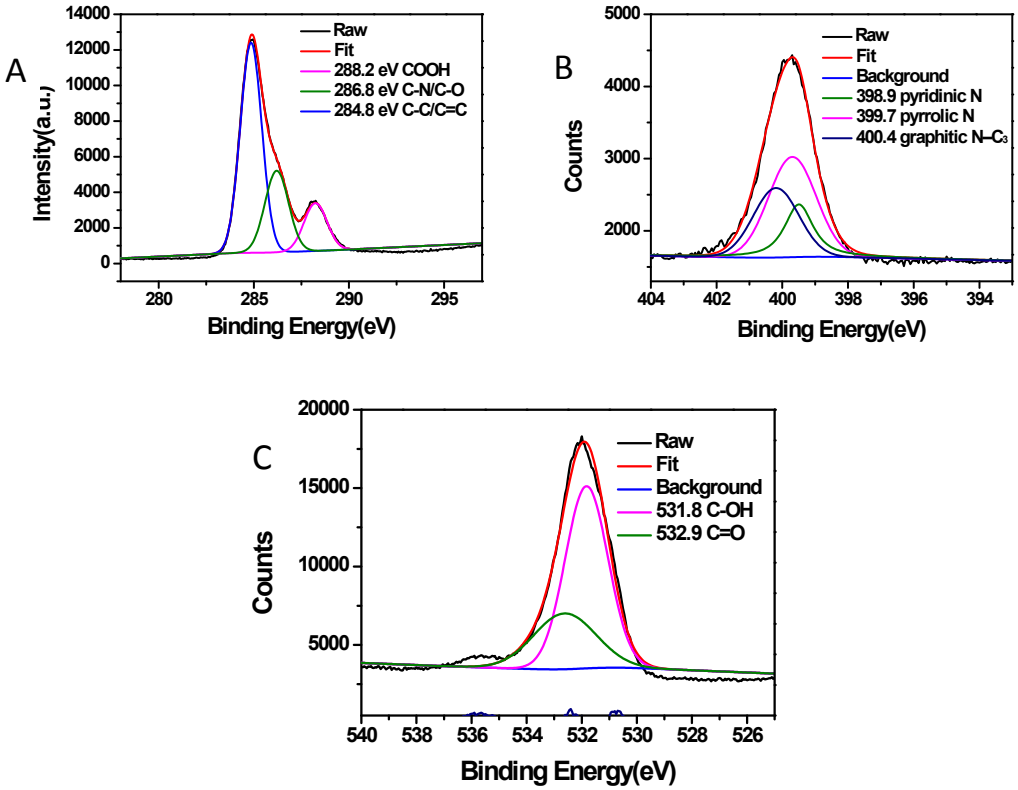

Fig. S1 High-resolution XPS data of C 1s (A), N 1s (B) , O1s (C) and P2p (D) of NCDs.

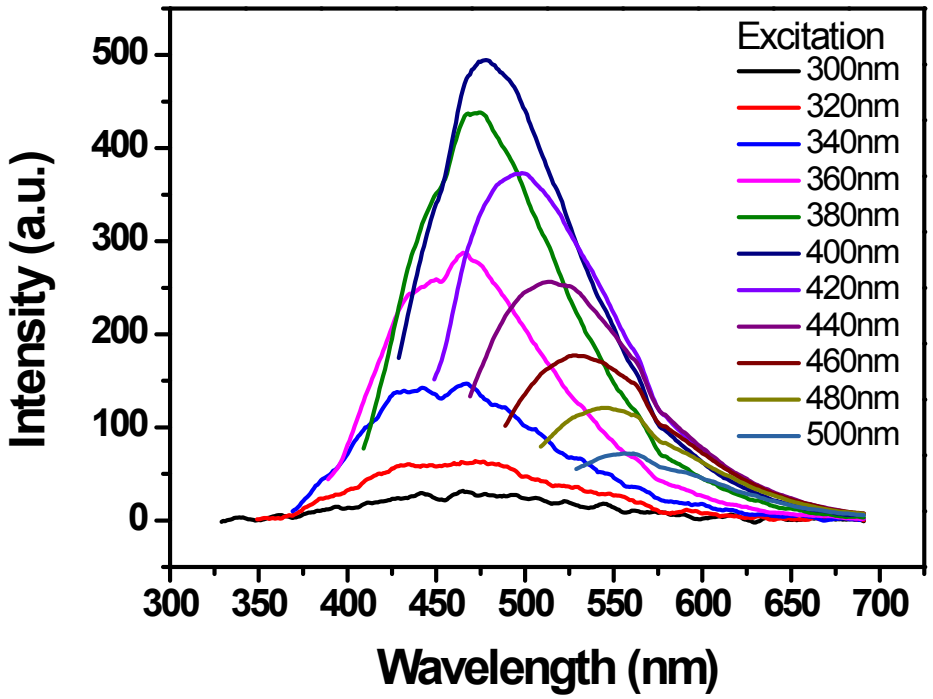

Fig. S2 FL emission spectra of the NCDs under different excitation wavelengths.

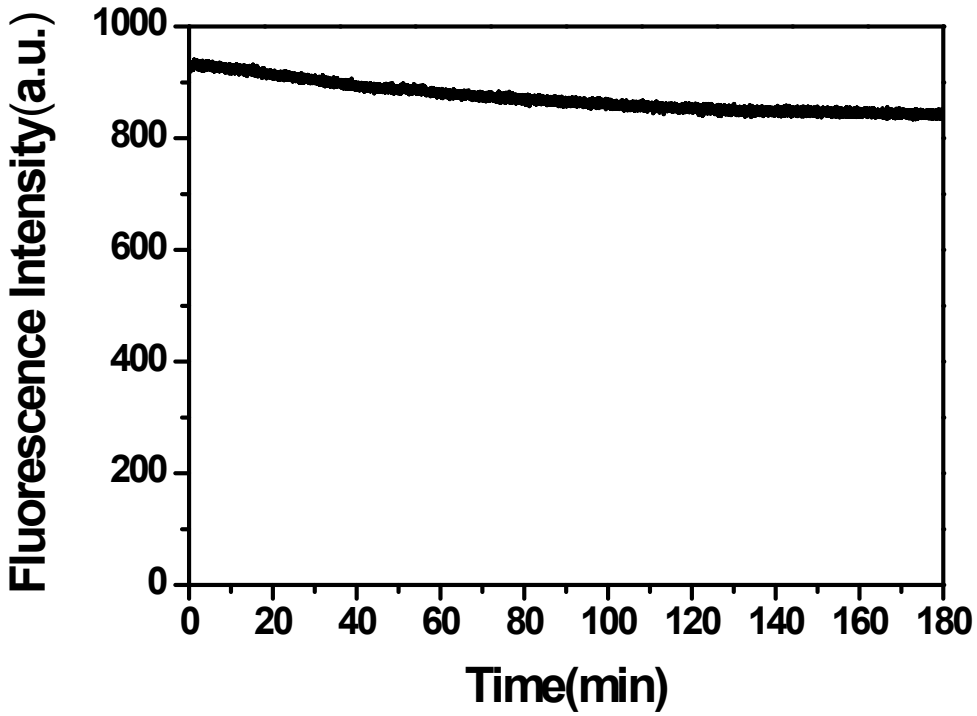

Fig. S3 Effect of time intervals of irradiation with xenon arc light on fluorescence intensity of NCDs.

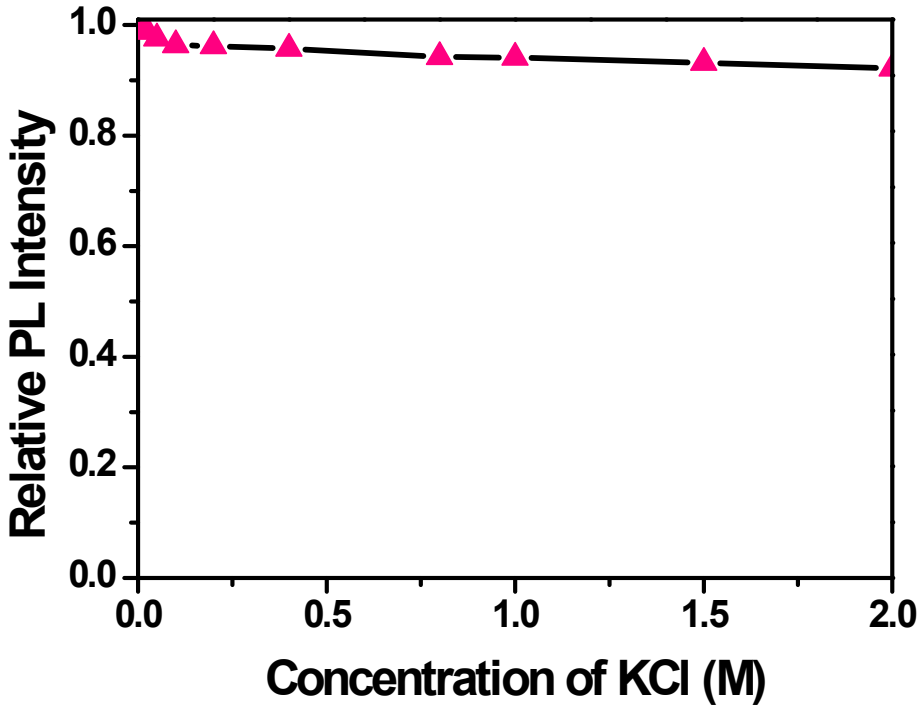

Fig. S4 Effect of ionic strength on fluorescence intensity of NCDs.

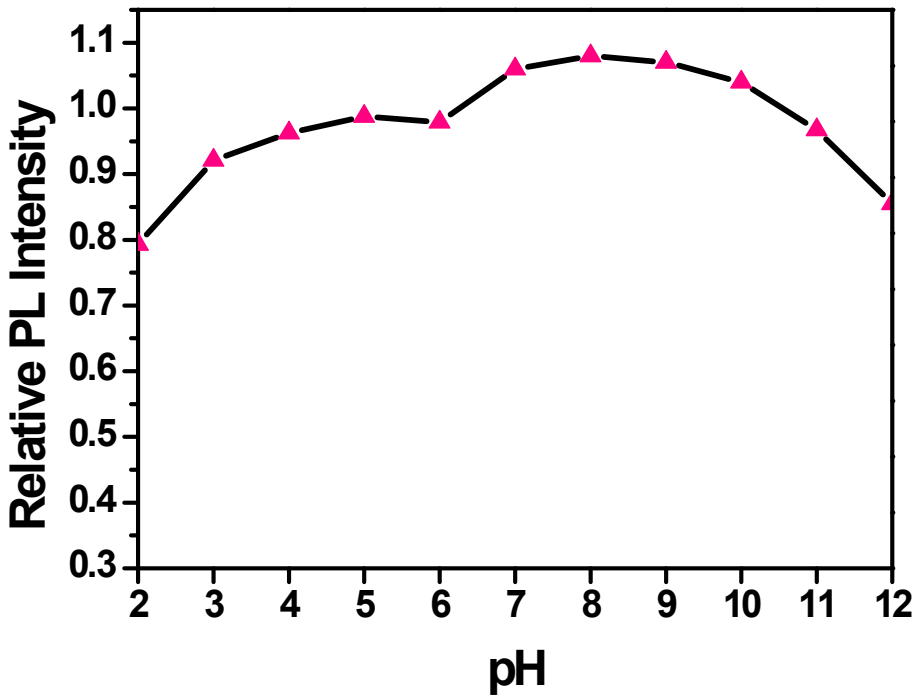

Fig. S5 The normalized fluorescence emission spectra of NCDs (0. 25 mg·mL^{-1}) at 475nm at different pH values.

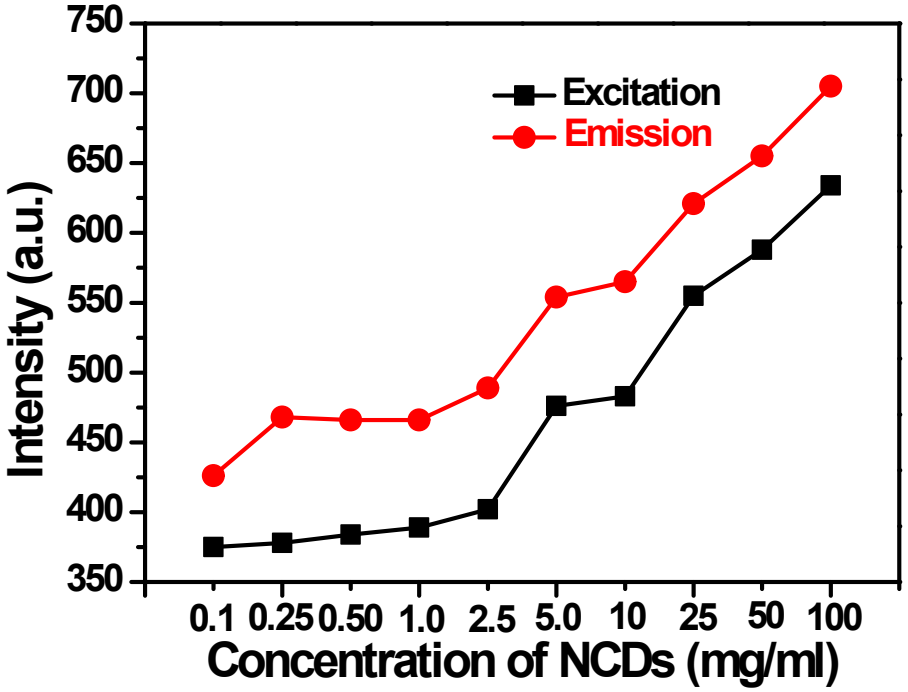

Fig. S6 Dependence of the maximum excitation wavelengths and maximum emission wavelengths on the concentration of NCDs.

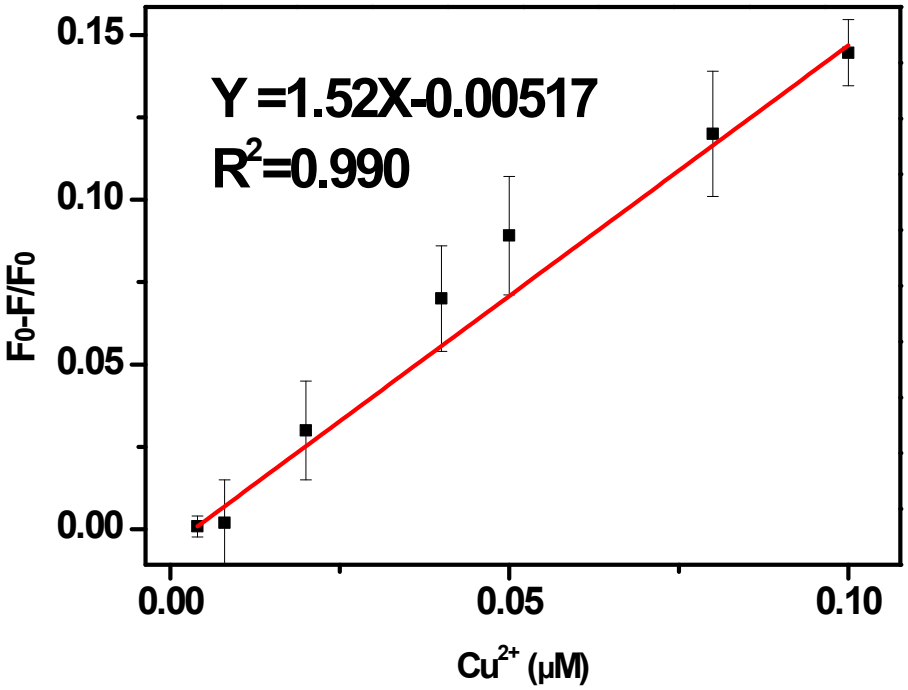

Fig. S7 The plot of NCDs to various concentrations of Cu^{2+} where F_0-F/F_0 are the PL intensities of NCDs in the absence and presence of Cu^{2+}, respectively.

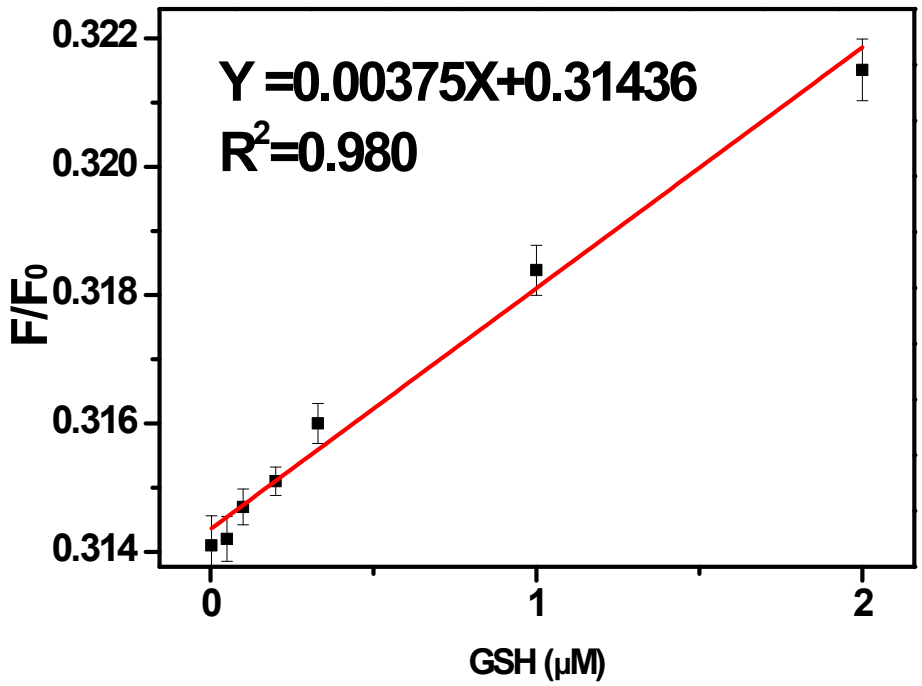

Fig. S8 The plot of NCDs to various concentrations of GSH where F_0/F are the PL intensities of NCDs-Cu^{2+} in the absence and presence of GSH, respectively.

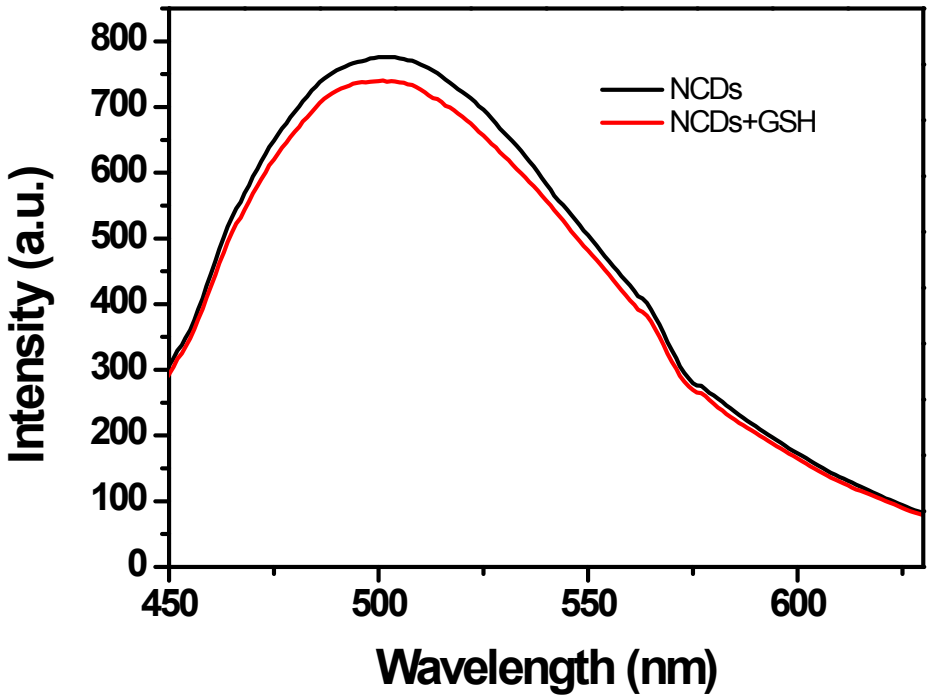

Fig. S9 The fluorescence of the NCDs and NCDs in the presence of GSH.

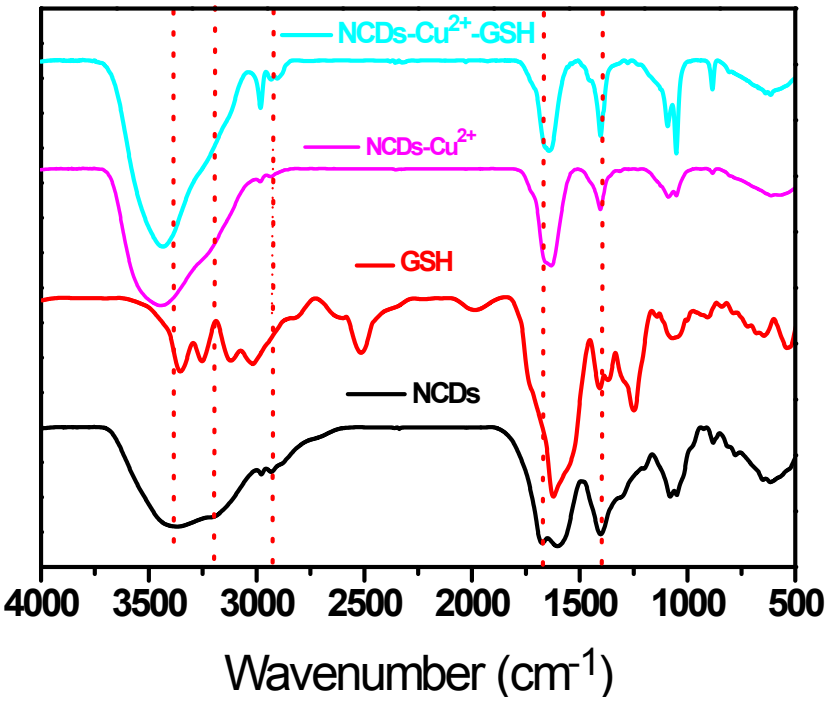

Fig. S10 The FT-IR spectrum of the NCDs, GSH, NCDs-Cu^{2+} and NCDs-Cu^{2+}-GSH.

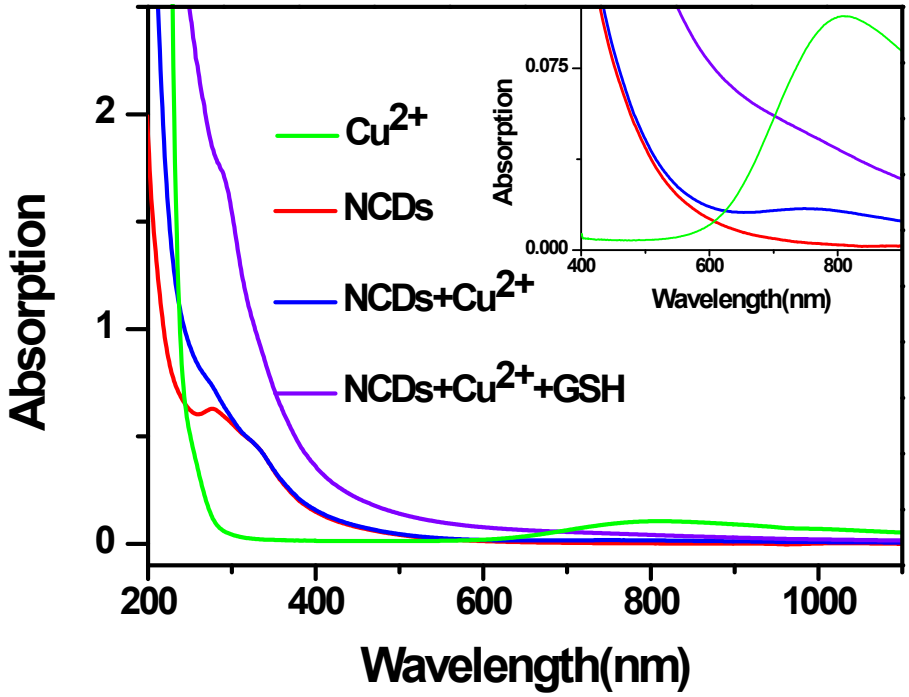

Fig. S11 The UV-vis spectrum of the NCDs, NCDs-Cu^{2+} and NCDs-Cu^{2+}-GSH.

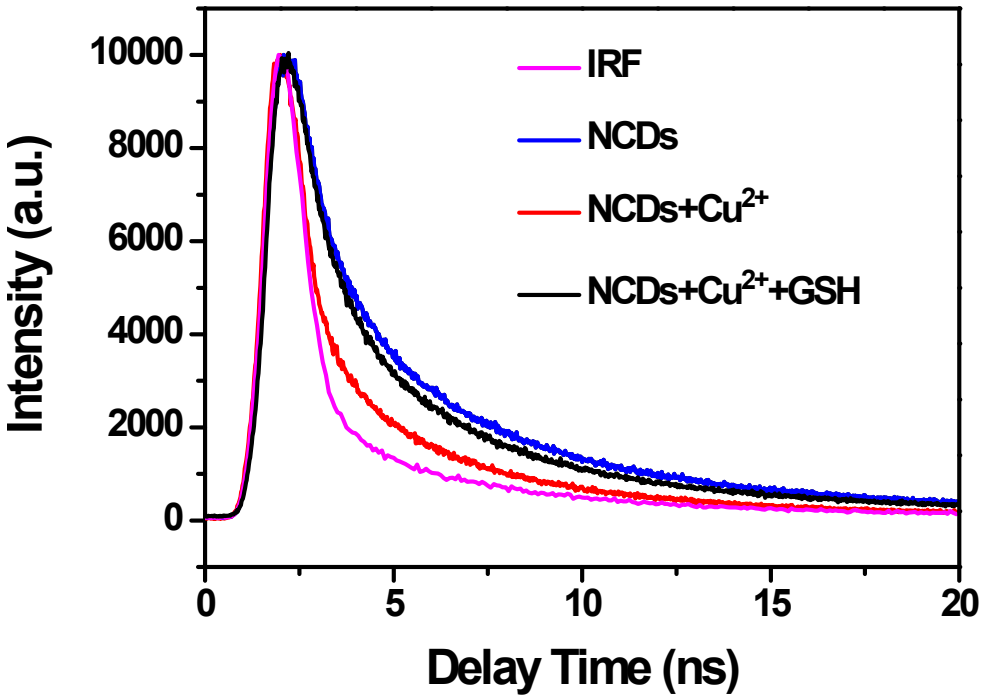

Fig. S12 Fluorescence decay lifetime of NCDs (0.50 mg/mL) without and with Cu^{2+} (10 mM) as a function of time at excitation/emission wavelengths (λex/λem) of 405/426 nm. IRF is the instrumental response function curve.

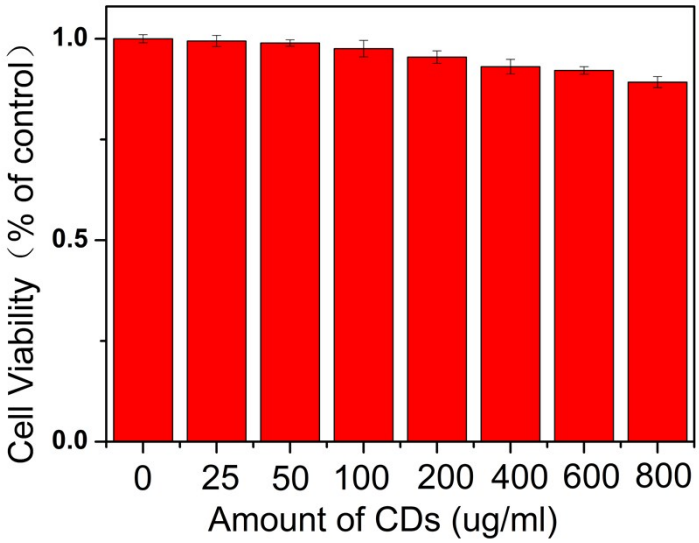

Fig. S13 Cytotoxicity test of NCDs on human liver cancer SMMC7721 viability. The values represent percentage cell viability (mean % ± SD, n = 6).

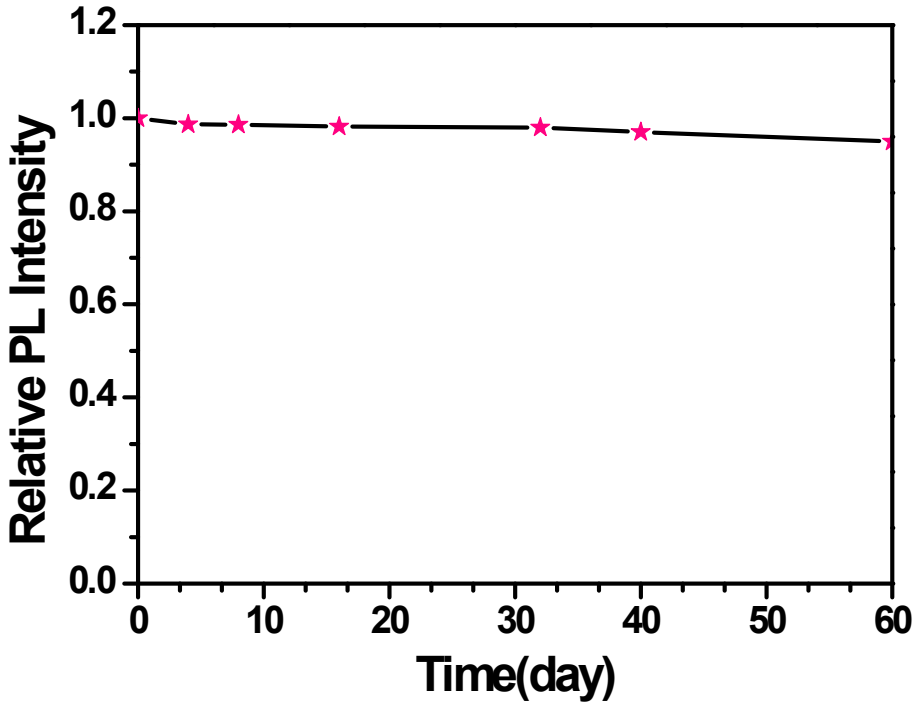

Fig. S14 The effect of exposure time under in air the intensity of fluorescence.

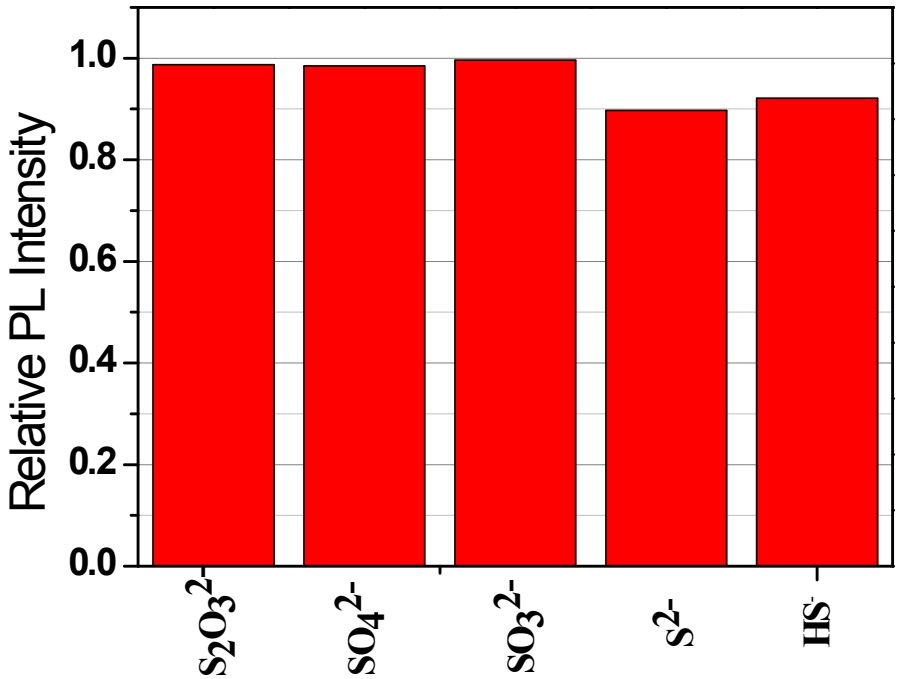

Fig. S15 The influence of H_2S and other anion on the relative fluorescence intensity of NCDs-Cu^{2+}.

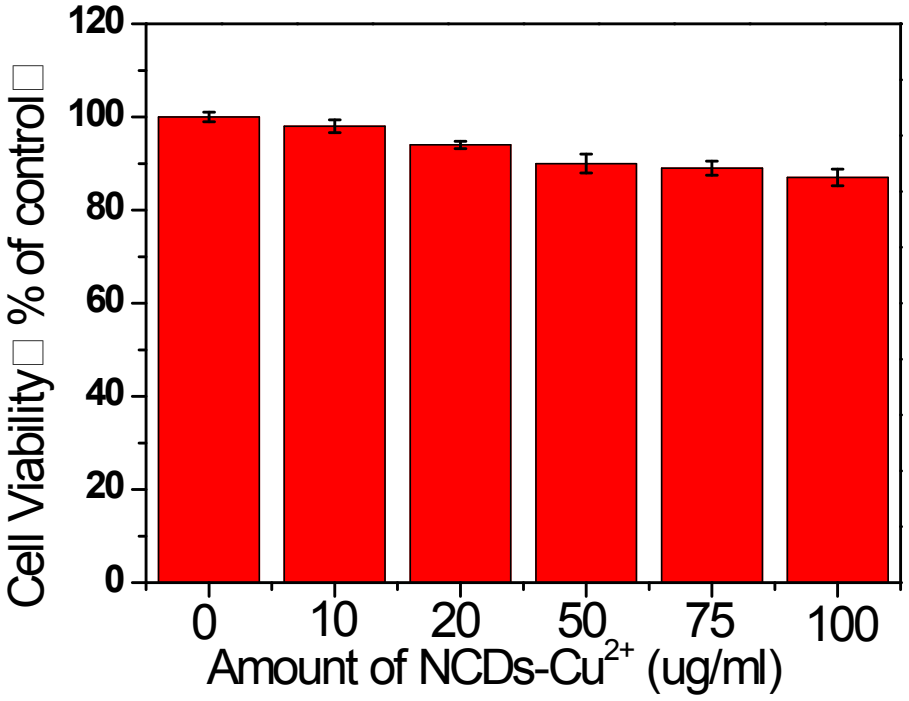

Fig. S16 Cytotoxicity test of NCDs-Cu^{2+} on human liver cancer SMMC7721 viability. The values represent percentage cell viability (mean % ± SD, n = 6).

1. Q. Qu, A. Zhu, X. Shao, G. Shi and Y. Tian, *Chemical Communications*, 2012, **48**, 5473-5475.
2. J. Chen, Y. Li, K. Lv, W. Zhong, H. Wang, Z. Wu, P. Yi and J. Jiang, *Sensors and Actuators B: Chemical*, 2016, **224**, 298-306.
3. H. Rao, W. Liu, Z. Lu, Y. Wang, H. Ge, P. Zou, X. Wang, H. He, X. Zeng and Y. Wang, *Microchimica Acta*, 2016, **183**, 581-588.
4. Y. Guo, L. Yang, W. Li, X. Wang, Y. Shang and B. Li, *Microchimica Acta*, 2016, **183**, 1409-1416.
5. J.-M. Liu, L.-p. Lin, X.-X. Wang, S.-Q. Lin, W.-L. Cai, L.-H. Zhang and Z.-Y. Zheng, *Analyst*, 2012, **137**, 2637-2642.
6. A. Salinas-Castillo, M. Ariza-Avidad, C. Pritz, M. Camprubi-Robles, B. Fernandez, M. J. Ruedas-Rama, A. Megia-Fernandez, A. Lapresta-Fernandez, F. Santoyo-Gonzalez, A. Schrott-Fischer and L. F. Capitan-Vallvey, *Chemical Communications*, 2013, **49**, 1103-1105.
7. G. Gedda, C.-Y. Lee, Y.-C. Lin and H.-f. Wu, *Sensors and Actuators B: Chemical*, 2016, **224**, 396-403.
8. P. Xu, C. Wang, D. Sun, Y. Chen and K. Zhuo, *Chemical Research in Chinese Universities*, 2015, **31**, 730-735.
9. Y. Lin, C. Wang, L. Li, H. Wang, K. Liu, K. Wang and B. Li, *ACS Applied Materials & Interfaces*, 2015, **7**, 27262-27270.
10. S. Wang, H. Ding, Y. Wang, C. Fan, G. Liu and S. Pu, *RSC Advances*, 2019, **9**, 6643-6649.
11. L. Meng, Z. Fang, J. Lin, M. Li and Z. Zhu, *Talanta*, 2014, **121**, 205-209.
12. X. Shao, H. Gu, Z. Wang, X. Chai, Y. Tian and G. Shi, *Analytical chemistry*, 2012, **85**, 418-425.

13. F. Wang, Y. Lu, Y. Chen, J. Sun and Y. Liu, *ACS Sustainable Chemistry & Engineering*, 2018, **6**, 3706-3713.
14. Z. Li, J. Zhang, Y. Li, S. Zhao, P. Zhang, Y. Zhang, J. Bi, G. Liu and Z. Yue, *Biosensors & bioelectronics*, 2018, **99**, 251-258.
15. Q.-Y. Cai, J. Li, J. Ge, L. Zhang, Y.-L. Hu, Z.-H. Li and L.-B. Qu, *Biosensors and Bioelectronics*, 2015, **72**, 31-36.
16. H. Fu, Z. Ji, X. Chen, A. Cheng, S. Liu, P. Gong, G. Li, G. Chen, Z. Sun and X. Zhao, *Analytical and bioanalytical chemistry*, 2017, **409**, 2373-2382.
17. D. Wu, G. Li, X. Chen, N. Qiu, X. Shi, G. Chen, Z. Sun, J. You and Y. Wu, *Microchimica Acta*, 2017, **184**, 1923-1931.